IEEE Access
Multidisciplinary | Rapid Review | Open Access Journal

SPECIAL SECTION ON INDEX MODULATION TECHNIQUES FOR NEXT-GENERATION WIRELESS NETWORKS

Received September 29, 2017, accepted October 26, 2017, date of publication November 13, 2017, date of current version December 5, 2017.

Digital Object Identifier 10.1109/ACCESS.2017.2771198

Performance of OFDM-IM Under Joint Hardware Impairments and Channel Estimation Errors Over Correlated Fading Channels

ASMA BOUHLEL[1], STAVROS G. DOMOUCHTSIDIS[2], SALAMA S. IKKI[3], AND ANIS SAKLY[4]

[1]Laboratory of Electronic and Microelectronic, Faculty of sciences Monastir, Monastir 5000, Tunisia
[2]Interdisciplinary Centre for Security, Reliability and Trust, Université du Luxembourg, L-1855 Luxembourg City, Luxembourg
[3]Electrical Engineering Department, Faculty of Engineering, Lakehead University, Thunder Bay, ON P7B 5E1, Canada
[4]Laboratory of Industrial systems study and renewable energy, National Engineering School of Monastir, Monastir 5000, Tunisia

Corresponding author: Asma Bouhlel (bouhlel_asmaa@yahoo.fr)

This work was supported in part by the Discovery Grant from the Natural Sciences and Engineering Research Council of Canada and in part by the Research Development Fund from Lakehead University.

ABSTRACT Recent studies have proven the potential of orthogonal frequency division multiplexing with index modulation in improving the bit error rate performance and the spectral efficiency, where its performance is evaluated under the assumption of ideal conditions. In this paper, the implementation of this novel transmission technique under realistic circumstances is thoroughly investigated. For this purpose, a new generalized system model that incorporates both imperfect channel state information and hardware impairments is employed and analytical pairwise error probability over correlated Rayleigh and Ricean fading channel is developed. The derived expression is then adapted to determine a tight upper bound of the average bit error probability. Furthermore, asymptotic expression analysis at high signal-to-noise ratio is included. Finally, simulation results are provided to illustrate the accuracy of the proposed theoretical analysis.

INDEX TERMS Orthogonal frequency division multiplexing, index modulation, non ideal channel estimation, hardware impairments, error probability analysis.

I. INTRODUCTION

Notable attention has been directed to Orthogonal Frequency Division Multiplexing with Index Modulation (OFDM-IM) as a dominant proposed solution to meet the major requirements of 5G systems. In fact, OFDM modulation divides the high serial data rate into parallel streams with low data rates, leading to low-complexity equalization by converting the frequency-selective channel into a set of parallel flat fading subchannels.

To further boost the spectral efficiency, index modulation, which is inspired by the concept of Spatial Modulation (SM), is joined to OFDM systems [1], [2]. Indeed, SM was inherently proposed for Multiple-Input Multiple-Output (MIMO) systems [3], [4]. The innovative idea in SM was to exploit the spatial dimension to enhance the data rate. In fact, the index of active transmit antenna is utilized to transfer additional data. By considering the subcarrier indices as antenna indices, the same idea of SM was readjusted for OFDM systems.

A recent study in [5] announced a novel modulation technique called OFDM with index modulation (OFDM-IM) as a robust key for wireless communication compared to techniques in [1] and [2]. The proposed idea of OFDM-IM systems in [5] is to implicitly employ the activated subcarrier index in carrying information in order to reach higher spectral efficiency use without increasing the modulation order. Furthermore, OFDM-IM system enhances the performance of traditional OFDM systems.

Similar to standard OFDM, the effects of channel estimation error and hardware impairments are dominant in the OFDM-IM performance degradation. However, for robust configuration of OFDM-IM under practical conditions, assuming the identical performance analysis when subject to imperfect channel state information (CSI) and hardware impairments, it will lead to inaccurate analysis.

For accurate detection in an OFDM-IM system, correct prediction of channel parameters is a crucial factor to consider. On the opposite side, erroneous knowledge of channel coefficients engenders performance degeneration [6]. Furthermore, estimation errors, aging and quantization errors are major causes of imperfect channel state

2169-3536 © 2017 IEEE. Translations and content mining are permitted for academic research only.
Personal use is also permitted, but republication/redistribution requires IEEE permission.
See http://www.ieee.org/publications_standards/publications/rights/index.html for more information.

information [7], [8]. Therefore, it is paramount to analyze the system behavior in the presence of imperfect channel state information before selecting the convenient channel estimation method [9], [10].

On the other hand, hardware can suffer from different kinds of impairment. Indeed, impairments are a result of the principle drawbacks of OFDM. For example, phase noise leading to orthogonality loss has a harmful effect on the system performance as mentioned in [11] and [12]. Moreover, OFDM signal presents high peak to average power ratio in time-domain, which causes performance sensitivity to nonlinearities, as described in [13] and [14]. Finally, I/Q imbalance in the RF front-end, creating limited matching, was mentioned in [15] and [16] as the major cause of performance deterioration.

To the best of the authors' knowledge, the performance evaluation of OFDM-IM under ideal conditions and in the presence of CSI was investigated in [5] over the special case of frequency selective Rayleigh fading channels. However, behavior analysis in the joint presence of CSI and nonideal hardware impairments over correlated Rayleigh and Rician fading channel have not been explored in the context of SM in general nor in OFDM-IM systems, specifically.

Motivated by the aforementioned limitations of the existing literature, this paper, based on optimum ML detector, studies the impact of the joint presence of channel estimation error and hardware impairments on OFDM-IM performance. Accordingly, a novel analytical expression of the pairwise error probability (PEP) under realistic conditions is proposed. The mentioned analytical approach leads to an upper bound on the average pairwise error probability and Average Bit Error Probability (ABEP) expressions over correlated Rayleigh and Ricean fading channel. In addition, these expressions are discussed to analyze the behavior of the system under different scenarios. The effectiveness of the proposed analytical approaches is confirmed through numerical simulations.

In this study, the OFDM-IM system model is first introduced. Subsequently, the analytical performances analysis for OFDM-IM that incorporates both imperfect channel state information and transceiver hardware impairments is developed in Section III. The efficiency of the suggested approach is then exhibited in the simulation results in Section IV. Finally, conclusions are given in Section V.

II. SYSTEM MODEL

The OFDM-IM system model as described in [5] is depicted in Fig. 1. Firstly, the M input data is turned into b bit parallel streams using G subblocks such as $M = bG$. Hence, each subblock is handling with $n = N/G$ subcarriers, where N denotes the orthogonal subcarriers. For the classical OFDM system, the total number of subcarriers are active and used to convey the modulated symbols. On the other hand, OFDM-IM uses only k out of n selected subcarriers that are active and their indices are defined using b_1 bits, while the sequence of b_2 bits is mapped over M-ary modulation.

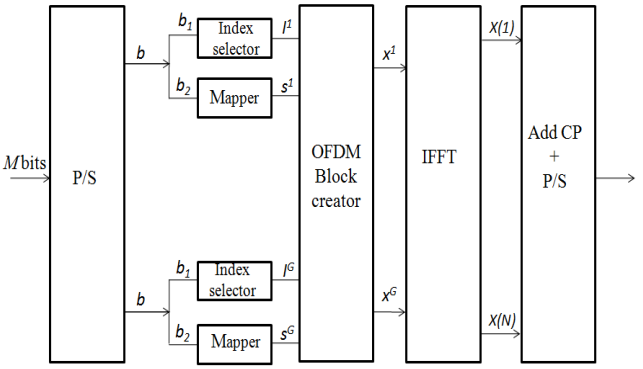

FIGURE 1. OFDM with index Modulation transmitter model as in [5].

Where $b_1 = \lfloor \log_2((C(n,k)) \rfloor$, with $C(n,k)$ denotes the binomial coefficient and $\lfloor . \rfloor$ is the integer floor operator, $b_2 = k \log_2(M)$ and $b = b_1 + b_2$. Thus, only k active subcarriers are carrying the mapped information and even their indices are used to transmit additional data, as shown in Fig. 2. The inactive subcarriers are not used for transmission and are set to zero.

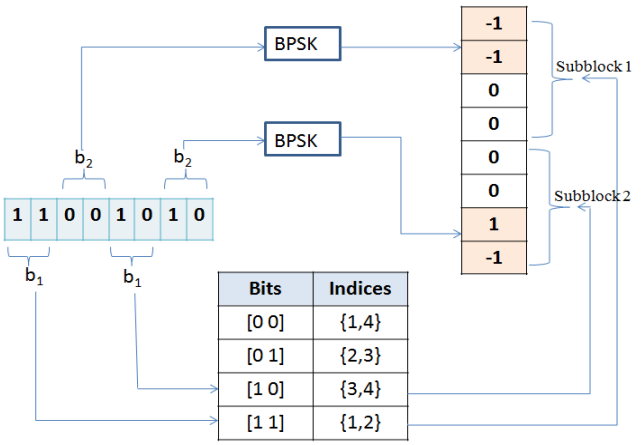

FIGURE 2. OFDM-IM modulator with $n = 4$, $k = 2$ and $G = 2$.

The indices of active subcarriers using the input sequence b_1 are determined from a look-up table known in the transmitter and receiver sides. As illustrated in Fig. 2, a possible set of selected indices are presented.

The indices of k active subcarriers defined by b_1 bit for the j^{th}subblock, are expressed as

$$I^j = \{I^j(1), \cdots, I^j(k)\}, \tag{1}$$

where $I^j(\epsilon) \in [1, \cdots, n]$ for $j = 1, \cdots, G$ and $\epsilon = 1, \cdots, k$. Furthermore, the transmitted data defined by b_2 input bit stream and mapped using M-ary modulation for the j^{th}subblock is described as

$$S^j = \{S^j(1), \cdots, S^j(k)\}, \tag{2}$$

where $j = 1, \cdots, G$.

Hence, the conveyed symbols over the selected active subcarriers for each subblock j can be given as

$$x^j = \begin{cases} S^j(\gamma), & \gamma \in I^j \\ 0 & \text{otherwise} \end{cases}. \tag{3}$$

Taking the example of the input bit sequence {1, 1, 0, 0}, for the j^{th} subblock using $n = 4$, $k = 2$ and Binary Phase Shift Keying (BPSK) modulation, $\lfloor \log_2(C(4,2)) \rfloor + 2\log_2(2)) = 4$ bits can be transmitted per OFDM-IM subblock. Considering the look-up table in Fig. 2, the active subcarriers indices can be selected as $I^j = \{1, 2\}$ as well the transmitted symbols vectors which are $S^j = \{-1, -1\}$. Thus, the resulting transmitted sequence is $x^j = \{-1, -1, 0, 0\}$.

After collecting the data from the subblocks, the Inverse Fast Fourier Transform (IFFT) is applied at the transmitter side to generate N parallel data streams. By applying IFFT, the symbol vectors are morphed into the time domain. To combat the effects of the Inter-Symbol Interference (ISI) conventional OFDM-IM based on FFT requires prepending a copy of the last part of each symbol. The signal is thereby fed through the channel vector $\boldsymbol{h}_t$ which is assumed to be the L multi-path complex Gaussian random vector. L is no higher than the cyclic prefix length. The added CP is removed from the signal vector at the receiver antenna and FFT is applied.

Without loss of generality, the received signal assuming ideal conditions can be expressed in the frequency domain for each subblock j as

$$\boldsymbol{y} = \sqrt{E}X\boldsymbol{h} + \boldsymbol{\eta}, \tag{4}$$

where $\boldsymbol{y} = [y^j(1) \cdots y^j(n)]^T$, E is the transmitted energy, $X = \text{diag}(x^j(1) \cdots x^j(n))$, is the transmitted data matrix and $\boldsymbol{h} = [h^j(1) \cdots h^j(n)]^T$ is the channel frequency response. Considering the fact that the FFT operation has been applied to the channel, $\boldsymbol{h}$ is also complex Gaussian vector, with mean of $\boldsymbol{h}_d$ and covariance matrix $C_h = \mathbb{E}\{(\boldsymbol{h} - \boldsymbol{h}_d)(\boldsymbol{h} - \boldsymbol{h}_d)^H\}$. Here, $\mathbb{E}\{.\}$ denotes the expectation and $\{.\}^H$ is the Hermitian operation which is the complex-conjugate transpose. Finally, $\boldsymbol{\eta} = [\eta^j(1) \cdots \eta^j(n)]^T$ is the distortion additive white Gaussian noise with zero mean and $N_{o,F}I_n$ variance in the frequency domain which is related to the noise variance in the time domain $N_{o,T}$ by $N_{o,F} = (kG/N)N_{o,T}$ [5]–[17].

To elaborate more on the channel gain, when the channel vector elements, $h^j(\ell)$, $\ell = 1, \cdots, n$, have zero mean, due to diffuse propagation, their absolute values, $|h^j(\ell)|$, have Rayleigh distribution. When the channel vector elements have a nonzero mean, due to specular propagation, their absolute values have Rician distribution. Propagation conditions determine the specular, i.e., deterministic, component $\boldsymbol{h}_d$ of the channel gain vector and the correlation matrix of the random component $\boldsymbol{h}_r$, i.e., $\boldsymbol{h} = \boldsymbol{h}_d + \boldsymbol{h}_r$.

For Rician fading, the K-factor is the power ratio of the deterministic (i.e., the mean) and random components of the channel gain. Assuming equal K for all indices, the channel gain vector can be written as

$$\boldsymbol{h} = \boldsymbol{h}_d + \boldsymbol{h}_r = \sqrt{\frac{K}{K+1}}\boldsymbol{h}_{dn} + \sqrt{\frac{1}{K+1}}\boldsymbol{h}_{rn}, \tag{5}$$

where, without loss of generality, the elements of $\boldsymbol{h}_{dn}$ and $\boldsymbol{h}_{rn}$ are assumed to be normalized, i.e., $|h^j_{dn}(\ell)| = 1$, $\mathbb{E}\{|h^j_{rn}(\ell)|^2\} = 1$, respectively, so that $\mathbb{E}\{|h^j(\ell)|^2\} = 1$. Therefore, the covariance matrix can be written as

$$C_{\boldsymbol{h}} = \mathbb{E}\{(\boldsymbol{h} - \boldsymbol{h}_d)(\boldsymbol{h} - \boldsymbol{h}_d)^H\} = \frac{1}{K+1}C_{\boldsymbol{h}_{rn}}, \tag{6}$$

where $C_{\boldsymbol{h}_{rn}} = \mathbb{E}\left\{\boldsymbol{h}_{rn}\boldsymbol{h}_{rn}^H\right\}$. Note that when $K = 0$ we have a Rayleigh fading channel.

At that point, the signal will be processed by the equalizer based on the optimal maximum likelihood (ML) detector for data recovery.

III. SYSTEM PERFORMANCE ANALYSIS

In the purpose of robust real implementation of the OFDM-IM system, a novel generalized system model is used to incorporate the effects of the joint presence of channel estimation error and hardware impairments. Hence, the received signal for the j^{th}subblock can be presented as

$$\boldsymbol{y} = \left[\sqrt{E}X + \boldsymbol{\omega}_t\right]\boldsymbol{h} + \boldsymbol{\omega}_r + \boldsymbol{\eta}, \tag{7}$$

where the effects of hardware impairments in the transmitter and receiver sides are characterized respectively by adding the following independent distortion noises $\boldsymbol{\omega}_t = \text{diag}\left([\omega^j_t(1), \cdots, \omega^j_t(n)]\right)$ and $\boldsymbol{\omega}_r = \text{diag}\left([\omega^j_r(1), \cdots, \omega^j_r(n)]\right)$.

Various exhaustive experiences have resulted that $\omega^j_t(\gamma) \sim \mathcal{CN}(0, \kappa_t^2 E)$ and $\omega^j_r(\gamma) \sim \mathcal{CN}(0, \kappa_r^2 E\left|h^j(\gamma)\right|^2)$ [18, Ch. 7], [19], [20]. The Gaussian distribution of the added distortion noises can be interpreted by the residual impact of impairments when using algorithms that eliminate all distinct types of distortions [21], [22].

In fact, κ_t^2 and κ_r^2 indicate the average of hardware impairments in transmitter and receiver sides [19], [23] which have typically small values in the range of [0, 0.03]. The above parameters can be measured in practice using the definition of the Error Vector Magnitude (EVM) as the ratio of the average distortion magnitude to the average signal magnitude [24]. Several studies have demonstrated that a small range of hardware impairments values is allowed to further boost the spectral efficiency.

Assuming the imperfect observation of the channel at the receiver, the estimated channel vector is defined as [5], [6]

$$\widetilde{\boldsymbol{h}} = \boldsymbol{h} + \boldsymbol{e}_h, \tag{8}$$

where $\boldsymbol{e}_h$ is the estimation error vector following a complex Gaussian random variable with zero mean and covariance $C_{\boldsymbol{e}_h} = \sigma_e^2 I_n$ and $\widetilde{\boldsymbol{h}}$ is the channel estimator vector assumed

to be complex Gaussian with mean $\boldsymbol{h}_d$ and covariance matrix as

$$\begin{aligned} C_{\widetilde{\boldsymbol{h}}} &= \mathbb{E}\left\{(\widetilde{\boldsymbol{h}}-\boldsymbol{h}_d)(\widetilde{\boldsymbol{h}}-\boldsymbol{h}_d)^H\right\} \\ &= \mathbb{E}\left\{(\boldsymbol{h}-\boldsymbol{h}_d+\boldsymbol{e}_h)(\boldsymbol{h}-\boldsymbol{h}_d+\boldsymbol{e}_h)^H\right\} \\ &= \frac{1}{K+1}C_{\boldsymbol{h}_m}+\sigma_e^2 I_n. \end{aligned} \tag{9}$$

Here it is assumed that the estimation error and estimated channel gain vectors are independent. The quality of the channel estimation is given by σ_e^2 value. In this model, pilot channel estimation sequences are used, which reduce the estimation errors linearly with increasing the number of pilots. In the case of perfect channel estimation $\sigma_e^2 = 0$.

In order to simplify the following derived expressions, and without loss of generality, a simplified general model for hardware impairments used in [25] and in [26] is adopted in this subsection. By introducing an aggregate distortion level $\kappa = \sqrt{\kappa_t^2+\kappa_r^2}$, without seperatly defining the effects of transmitter hardware κ_t and the receiver hardware κ_r, (7) becomes

$$\boldsymbol{y} = (\sqrt{E}X+\boldsymbol{\omega})\boldsymbol{h}+\boldsymbol{\eta}, \tag{10}$$

where $\boldsymbol{\omega} = \text{diag}([\omega^j(1),\cdots,\omega^j(n)])$ is the independent distortion noise which diagonal elements follow the $CN(0,\kappa^2 E)$ distribution and models the hardware impairments at both the transmitter and the receiver. For ideal hardware case $\kappa^2 = 0$.

Using (8) and (10), the received signal affected by the joint presence of hardware impairments and channel estimation error for each subblock j becomes

$$\begin{aligned} \boldsymbol{y} &= (\sqrt{E}X+\boldsymbol{\omega})\boldsymbol{h}+\boldsymbol{\eta} \\ &= \sqrt{E}X\widetilde{\boldsymbol{h}}+\sqrt{E}X\boldsymbol{e}_h+\boldsymbol{\omega}\widetilde{\boldsymbol{h}}+\boldsymbol{\omega}\boldsymbol{e}_h+\boldsymbol{\eta}. \end{aligned} \tag{11}$$

A joint search for the active subcarriers and symbol sequence for each subblock is concluded by ML detector. In particular, a detector estimates the complex channel gains as in equation (8) and uses the result in the same metric that would be applied if the channel were perfectly known. Given that the transmitted symbols are assumed equally likely, the optimal detector can be expressed as

$$[\hat{X}]_{\text{ML}} = \arg\min_X \left\|\boldsymbol{y}-\sqrt{E}X\widetilde{\boldsymbol{h}}\right\|^2. \tag{12}$$

A. CONDITIONAL PAIRWISE ERROR PROBABILITY

Assuming X is transmitted vector, the probability of deciding in favor of $\widehat{X}$ is given from (12) as

$$\begin{aligned} &\text{PEP} \\ &= Pr\left(X\to\widehat{X}|\widetilde{\boldsymbol{h}}\right) \\ &= \text{P}_\text{r}\left(\left\|\boldsymbol{y}-\sqrt{E}X\widetilde{\boldsymbol{h}}\right\|^2 > \left\|\boldsymbol{y}-\sqrt{E}\widehat{X}\widetilde{\boldsymbol{h}}\right\|^2\right) \\ &= \text{P}_\text{r}\left(\left\|\sqrt{E}X\boldsymbol{e}_h+\boldsymbol{\omega}\widetilde{\boldsymbol{h}}+\boldsymbol{\omega}\boldsymbol{e}_h+\boldsymbol{\eta}\right\|^2\right. \\ &\qquad \left. > \left\|\sqrt{E}(X-\widehat{X})\widetilde{\boldsymbol{h}}+\sqrt{E}X\boldsymbol{e}_h+\boldsymbol{\omega}\widetilde{\boldsymbol{h}}+\boldsymbol{\omega}\boldsymbol{e}_h+\boldsymbol{\eta}\right\|^2\right) \\ &= \text{P}_\text{r}\left(\left\|\sqrt{E}(X-\widehat{X})\widetilde{\boldsymbol{h}}\right\|^2\right. \\ &\qquad \left. < -2\Re\left\{(\sqrt{E}X\boldsymbol{e}_h+\boldsymbol{\omega}\widetilde{\boldsymbol{h}}+\boldsymbol{\omega}\boldsymbol{e}_h+\boldsymbol{\eta})^H\sqrt{E}(X-\widehat{X})\widetilde{\boldsymbol{h}}\right\}\right) \\ &= \text{P}_\text{r}\left(\lambda > \left\|\sqrt{E}(X-\widehat{X})\widetilde{\boldsymbol{h}}\right\|^2\right), \end{aligned} \tag{13}$$

where $\Re\{z\}$ denotes the real part of the complex number z and

$$\begin{aligned} \lambda &= 2\Re\left\{E\boldsymbol{e}_h^H X^H(X-\widehat{X})\widetilde{\boldsymbol{h}}+\sqrt{E}\widetilde{\boldsymbol{h}}^H\boldsymbol{\omega}^H(X-\widehat{X})\widetilde{\boldsymbol{h}}\right. \\ &\qquad \left.+\sqrt{E}\boldsymbol{e}_h^H\boldsymbol{\omega}^H(X-\widehat{X})\widetilde{\boldsymbol{h}}+\sqrt{E}\boldsymbol{\eta}^H(X-\widehat{X})\widetilde{\boldsymbol{h}}\right\} \\ &= 2\Re\{\zeta+\theta+\phi+\Omega\}, \end{aligned} \tag{14}$$

where

$$\begin{cases} \zeta = E\boldsymbol{e}_h^H X^H(X-\widehat{X})\widetilde{\boldsymbol{h}}, \\ \theta = \sqrt{E}\widetilde{\boldsymbol{h}}^H\boldsymbol{\omega}^H(X-\widehat{X})\widetilde{\boldsymbol{h}}, \\ \phi = \sqrt{E}\boldsymbol{e}_h^H\boldsymbol{\omega}^H(X-\widehat{X})\widetilde{\boldsymbol{h}}, \\ \Omega = \sqrt{E}\boldsymbol{\eta}^H(X-\widehat{X})\widetilde{\boldsymbol{h}}. \end{cases} \tag{15}$$

Note that ϕ is not a Gaussian variable since it involves multiplication of two Gaussian random variables. However, taking the premise of small levels of estimation error and hardware impairments in practice cases, a tight approximation such as $\boldsymbol{e}_h^H\boldsymbol{\omega}^H \sim \mathcal{CN}(0,\kappa^2 E\sigma_e^2 I_n)$ could be allowed without losing the accuracy of the coming analysis.

Moreover, using the mutual independency among ζ, θ and Ω, λ conditioned on $\widetilde{\boldsymbol{h}}$ is considered a Gaussian random variable and its expectation and variance are respectively derived as

$$\mathbb{E}\{\lambda\} = 2\left(\mathbb{E}\{\zeta\}+\mathbb{E}\{\theta\}+\mathbb{E}\{\phi\}+\mathbb{E}\{\Omega\}\right) = 0, \tag{16}$$

$$Var(\lambda) = 2\left(\mathbb{E}\{\zeta\zeta^H\}+\mathbb{E}\{\theta\theta^H\}+\mathbb{E}\{\phi\phi^H\}+\mathbb{E}\{\Omega\Omega^H\}\right), \tag{17}$$

where $Var\{.\}$ denotes the variance operations.

To calculate (17), it can be proceeded by

$$\begin{aligned} \mathbb{E}\{\zeta\zeta^H\} &= \mathbb{E}\{E^2\boldsymbol{e}_h^H X^H(X-\widehat{X})\widetilde{\boldsymbol{h}}\widetilde{\boldsymbol{h}}^H(X-\widehat{X})^H X\boldsymbol{e}_h\} \\ &= E^2\sigma_e^2\left\|X^H(X-\widehat{X})\widetilde{\boldsymbol{h}}\right\|^2, \end{aligned} \tag{18}$$

The second term in (15) can be computed as

$$\begin{aligned} \mathbb{E}\{\theta\theta^H\} &= \mathbb{E}\{E\widetilde{\boldsymbol{h}}^H\boldsymbol{\omega}^H(X-\widehat{X})\widetilde{\boldsymbol{h}}\widetilde{\boldsymbol{h}}^H(X-\widehat{X})^H\boldsymbol{\omega}\widetilde{\boldsymbol{h}}\} \\ &= E^2\kappa^2\left\|\widetilde{\boldsymbol{h}}^H(X-\widehat{X})\widetilde{\boldsymbol{h}}\right\|^2. \end{aligned} \tag{19}$$

To find the previous results, it is worth noting that $(X-\widehat{X})\widetilde{\boldsymbol{h}}\widetilde{\boldsymbol{h}}^H(X-\widehat{X})^H$ is a diagonal matrix with $n\times n$ dimension and $\left|x^j(\gamma)-\widehat{x}^j(\gamma)\right|^2\left|\widetilde{h}^j(\gamma)\right|^2$ are the diagonal elements.

On the other side, the variance of ϕ can be defined as

$$\begin{aligned} \mathbb{E}\{\phi\phi^H\} &= \mathbb{E}\{E\boldsymbol{e}_h^H\boldsymbol{\omega}^H(X-\widehat{X})\widetilde{\boldsymbol{h}}\widetilde{\boldsymbol{h}}^H(X-\widehat{X})^H\boldsymbol{\omega}\boldsymbol{e}_h\} \\ &= E^2\kappa^2\sigma_e^2\left\|(X-\widehat{X})\widetilde{\boldsymbol{h}}\right\|^2. \end{aligned} \tag{20}$$

Finally, $\mathbb{E}\{\Omega\Omega^H\}$ can be calculated as

$$\mathbb{E}\{\Omega\Omega^H\} = EN_{0F}\left\|(X-\widehat{X})\widetilde{\boldsymbol{h}}\right\|^2. \tag{21}$$

$$\Pr\left(X\to\widehat{X}|\widetilde{\boldsymbol{h}}\right)=Q\left(\sqrt{\frac{E\left\|(X-\widehat{X})\widetilde{\boldsymbol{h}}\right\|^4}{2E\sigma_e^2\left\|X^H(X-\widehat{X})\widetilde{\boldsymbol{h}}\right\|^2+2E\kappa^2\left\|\widetilde{\boldsymbol{h}}^H(X-\widehat{X})\widetilde{\boldsymbol{h}}\right\|^2+2E\kappa^2\sigma_e^2\left\|(X-\widehat{X})\widetilde{\boldsymbol{h}}\right\|^2+2N_{0F}\left\|(X-\widehat{X})\widetilde{\boldsymbol{h}}\right\|^2}}\right). \quad (23)$$

Using the above results, (17) can be written as

$$\sigma_\lambda^2\approx 2E^2\sigma_e^2\left\|X^H(X-\widehat{X})\widetilde{\boldsymbol{h}}\right\|^2+2E^2\kappa^2\left\|\widetilde{\boldsymbol{h}}^H(X-\widehat{X})\widetilde{\boldsymbol{h}}\right\|^2 +2E^2\kappa^2\sigma_e^2\left\|(X-\widehat{X})\widetilde{\boldsymbol{h}}\right\|^2+2EN_{0F}\left\|(X-\widehat{X})\widetilde{\boldsymbol{h}}\right\|^2. \quad (22)$$

Based on (22), the conditional PEP under the joint presence of channel estimation error and hardware impairments is determined in (23) on the top of this page, where $Q(x)$ denotes the Q-function defined as $Q(x)=\frac{1}{2\pi}\int_x^\infty\exp(\frac{-x^2}{2})dx$. It is obviously seen that imperfect estimation and/or hardware impairments degrades the system performance. Note that when $\kappa=0$ and $\sigma_e^2=0$, the conditional PEP can be greatly simplified to

$$\Pr\left(X\to\widehat{X}|\widetilde{\boldsymbol{h}}\right)=Q\left(\sqrt{\frac{E\left\|(X-\widehat{X})\boldsymbol{h}\right\|^2}{2N_{0F}}}\right). \quad (24)$$

B. AVERAGE PAIRWISE ERROR PROBABILITY

In the attempt to provide a more adequate theoretical performance description, tight approximations will be provided. Recall that it has been assumed X is with a unitary energy, the following inequality can be modified as

$$\left\|X^H(X-\widehat{X})\widetilde{\boldsymbol{h}}\right\|^2\le\left\|X^H\right\|^2\left\|(X-\widehat{X})\widetilde{\boldsymbol{h}}\right\|^2 =\left\|(X-\widehat{X})\widetilde{\boldsymbol{h}}\right\|^2. \quad (25)$$

Furthermore, the following matrices simplification is used

$$E^2\kappa^2\left\|\widetilde{\boldsymbol{h}}^H(X-\widehat{X})\widetilde{\boldsymbol{h}}\right\|^2=E^2\kappa^2\sum_{\gamma=1}^{n}\left|x^j(\gamma)-\widehat{x}^j(\gamma)\right|^2\times\left|\widetilde{h}^j(\gamma)\right|^2\left|\widetilde{h}^j(\gamma)\right|^2 \le E^2\kappa^2\left\|(X-\widehat{X})\widetilde{\boldsymbol{h}}\right\|^2. \quad (26)$$

Accordingly, the upper bound on the conditional PEP under the above conditions can be simplified to

$$\Pr\left(X\to\widehat{X}|\widetilde{\boldsymbol{h}}\right)\le Q\left(\sqrt{\frac{E\left\|(X-\widehat{X})\widetilde{\boldsymbol{h}}\right\|^2}{2E\sigma_e^2+2E\kappa^2+2E\kappa^2\sigma_e^2+2N_{0F}}}\right). \quad (27)$$

Using the expression of signal-to-noise ratio in the frequency domain $\mathbf{SNR_F}=\frac{E}{N_{o,F}}$, (27) can be rewritten as

$$\Pr\left(X\to\widehat{X}|\widetilde{\boldsymbol{h}}\right)\le Q\left(\sqrt{\frac{\mathbf{SNR_F}\left\|(\mathbf{X}-\widehat{\mathbf{X}})\widetilde{\boldsymbol{h}}\right\|^2}{2(\mathbf{SNR_F}\sigma_{\mathbf{e}}^2+\mathbf{SNR_F}\kappa^2+\mathbf{SNR_F}\kappa^2\sigma_{\mathbf{e}}^2+\mathbf{1})}}\right). \quad (28)$$

Noting that

$$\left\|(X-\widehat{X})\widetilde{\boldsymbol{h}}\right\|^2=\widetilde{\boldsymbol{h}}^H(X-\widehat{X})^H(X-\widehat{X})\widetilde{\boldsymbol{h}} =\left((X-\widehat{X})\widetilde{\boldsymbol{h}}\right)^H\left((X-\widehat{X})\widetilde{\boldsymbol{h}}\right) =\boldsymbol{\psi}^H\boldsymbol{\psi}, \quad (29)$$

where $\boldsymbol{\psi}=(X-\widehat{X})\widetilde{\boldsymbol{h}}$ is a complex Gaussian vector with mean $(X-\widehat{X})h_d$ and covariance matrix defined using (9) as

$$C_{\boldsymbol{\psi}}=\mathbb{E}\{[\boldsymbol{\psi}-(X-\widehat{X})h_d][\boldsymbol{\psi}-(X-\widehat{X})h_d]^H\} =(X-\widehat{X})C_{\widetilde{\boldsymbol{h}}}(X-\widehat{X})^H =\frac{1}{K+1}(X-\widehat{X})C_{\boldsymbol{h}_m}(X-\widehat{X})^H. \quad (30)$$

Thus, the conditional pairwise error probability given in (28) can be expressed as

$$\Pr\left(X\to\widehat{X}|\widetilde{\boldsymbol{h}}\right)\le Q\left(\sqrt{2\mu\boldsymbol{\psi}^H\boldsymbol{\psi}}\right)=Q\left(\sqrt{2\varphi}\right), \quad (31)$$

where

$$\mu=\frac{\mathbf{SNR_F}}{4(\mathbf{SNR_F}\sigma_{\mathbf{e}}^2+\mathbf{SNR_F}\kappa^2+\mathbf{SNR_F}\kappa^2\sigma_{\mathbf{e}}^2+\mathbf{1})},$$

and $\varphi=\mu\boldsymbol{\psi}^H\boldsymbol{\psi}$. Since φ is in quadratic form as in [27], and the Q-function can be alternatively expressed as [28]

$$Q(x)=\frac{1}{\pi}\int_0^{\frac{\pi}{2}}\exp\left(\frac{-x^2}{2\sin^2\theta}\right)d\theta. \quad (32)$$

To calculate the unconditional pairwise error $\overline{\text{PEP}}$, (31) should be averaged over the Probability Density Function (PDF) of $\boldsymbol{\psi}$. The PDF of $\boldsymbol{\psi}$ can be depicted as [29]

$$f(\psi)=\frac{\pi^{-n}}{\det(C_{\boldsymbol{\psi}})}\exp\left(-[\boldsymbol{\psi}-(X-\widehat{X})\boldsymbol{h}_d]^H\times C_{\boldsymbol{\psi}}^{-1}[\boldsymbol{\psi}-(X-\widehat{X})\boldsymbol{h}_d]\right). \quad (33)$$

Using (32) and (33), the average pairwise error probability can be written as

$$\overline{\text{PEP}}\le\frac{1}{\pi}\int_{\boldsymbol{\psi}}\int_0^{\frac{\pi}{2}}\exp\left(\frac{-\mu\boldsymbol{\psi}^H\boldsymbol{\psi}}{\sin^2\theta}\right)\frac{\pi^{-n}}{\det(C_{\boldsymbol{\psi}})} \times\exp\left(-(\boldsymbol{\psi}-(X-\widehat{X})\boldsymbol{h}_d)^HC_{\boldsymbol{\psi}}^{-1}(\boldsymbol{\psi}-(X-\widehat{X})\boldsymbol{h}_d)\right)d\theta d\boldsymbol{\psi}. \quad (34)$$

Exploiting the property of Hermitian and using the assumption that a proper complex Gaussian (PCG) joint pdf

$$\overline{\text{PEP}} \leq \frac{1}{\pi}\int_0^{\frac{\pi}{2}} \left[\det\left(\frac{\mu}{\sin^2\theta}(X-\widehat{X})\left(\frac{1}{K+1}C_{\boldsymbol{h}_{rn}}+\sigma_e^2 I_n\right)(X-\widehat{X})^H + I_n\right)\right]^{-1} \times \exp\left(\frac{-K}{(K+1)}\boldsymbol{h}_{dn}^H(X-\widehat{X})^H\left(\frac{1}{(K+1)}C_{\boldsymbol{h}_{rn}}+\sigma_e^2 I_n+\frac{\sin^2\theta}{\mu}I_n\right)^{-1}(X-\widehat{X})\boldsymbol{h}_{dn}\right) d\theta. \quad (36)$$

$$\overline{\text{PEP}} \approx \frac{\exp\left(\frac{-K}{(K+1)}\boldsymbol{h}_{dn}^H(X-\widehat{X})^H\left(\frac{1}{(K+1)}C_{\boldsymbol{h}_{rn}}+\sigma_e^2 I_n+\frac{1}{\mu}I_n\right)^{-1}(X-\widehat{X})\boldsymbol{h}_{dn}\right)}{2\det\left(\mu(X-\widehat{X})\left(\frac{1}{K+1}C_{\boldsymbol{h}_{rn}}+\sigma_e^2 I_n\right)(X-\widehat{X})^H+I_n\right)}. \quad (37)$$

integrates to one, the above expression can be calculated as

$$\overline{\text{PEP}} \leq \frac{1}{\pi}\int_0^{\frac{\pi}{2}}\left[\det\left(\frac{\mu C_{\boldsymbol{\psi}}}{\sin^2\theta}+I_n\right)\right]^{-1} \exp\left(-\boldsymbol{h}_d^H(X-\widehat{X})^H\left(C_{\boldsymbol{\psi}}+\frac{\sin^2\theta}{\mu}I_n\right)^{-1}(X-\widehat{X})\boldsymbol{h}_d\right) d\theta, \quad (35)$$

where I_n refers to the $n \times n$ identity matrix. The above expression is evaluated depending on $\boldsymbol{h}_d$ value, hence the channel model.

1) RICIAN FADING CHANNEL

In such case, $\boldsymbol{h}_d \neq 0$. Substituting $C_{\boldsymbol{\psi}}$ in (35) by (30), the average pairwise error probability can be expressed as in (36) on the top of this page.

Consequently, (36) cannot be further simplified and the exponential polynomial can not be removed from the integration. However, it can be numerically evaluated for any given K using the fact that (36) is a single finite-range integral, with an integrand that is a ratio of polynomials of trigonometric functions [29]. However, the above integration can be approximated (by letting $\sin\theta = 1$) as noted on the top of the next page.

Two interesting points can be observed from the above expression. First, in high $\mathbf{SNR_F}$, the line-of-sight component offers a fixed coding gain, but no diversity advantage. Second, as K approached infinity, i.e., the channel approaches additive white Gaussian noise channel (AWGN), the $\overline{\text{PEP}}$ approaches the error in AWGN channel, which validates the provided analysis.

2) RAYLEIGH FADING CHANNEL

For Rayleigh fading case, $\boldsymbol{h}_d = 0$ (or $K = 0$) then (35) is reduced to

$$\overline{\text{PEP}} \leq \frac{1}{\pi}\int_0^{\frac{\pi}{2}}\left[\det\left(\frac{\mu C_{\boldsymbol{\psi}}}{\sin^2\theta}+I_n\right)\right]^{-1} d\theta. \quad (38)$$

By considering $\lambda_{g,g=1,\ldots,r}$ as the distinct eigenvalues set of the matrix matrix $C_{\boldsymbol{\psi}}$ of rank r, the expression in (38) can be rewritten as

$$\overline{\text{PEP}} \leq \sum_{g=1}^{r}\prod_{i\neq g}\left(1-\frac{\lambda_i}{\lambda_g}\right)^{-1}\int_0^{\frac{\pi}{2}}\left(\frac{\sin^2\theta}{\sin^2\theta+\mu\lambda_g}\right)d\theta. \quad (39)$$

A closed form expression for the above integral is given in [31, Appendix B], hence, the expression in (39) can be integrated as

$$\overline{\text{PEP}} \approx \frac{1}{2}\sum_{g=1}^{r}\prod_{i\neq g}\left(1-\frac{\lambda_i}{\lambda_g}\right)^{-1}\left[1-\sqrt{\frac{\mu\lambda_g}{1+\mu\lambda_g}}\right]. \quad (40)$$

C. ASYMPTOTIC PERFORMANCE ANALYSIS

To further evaluate the impact of channel estimation error and the hardware impairments on the OFDM-IM system, first, we consider the Rayleigh channel and later on we generalize the analysis for Rician Channel.

The upper bound PEP in (37), as shown at the top of this page, is thus approximated at high $\mathbf{SNR_F}$ values for Rayleigh fading channel as

$$\overline{\text{PEP}} \approx \frac{1}{2\det\left(\mu(X-\widehat{X})\left(\frac{1}{K+1}C_{\boldsymbol{h}_{rn}}+\sigma_e^2 I_n\right)(X-\widehat{X})^H+I_n\right)}. \quad (41)$$

Supposing $B = (X-\widehat{X})\left(\frac{1}{K+1}C_{\boldsymbol{h}_{rn}}+\sigma_e^2 I_n\right)(X-\widehat{X})^H$ has distinct eigenvalues $\lambda_1, \cdots, \lambda_r$, hence (41) can be rewritten as

$$\overline{\text{PEP}} \approx \left(2\prod_{g=1}^{r}(1+\mu\lambda_g)\right)^{-1}. \quad (42)$$

Taking the assumption of high $\mathbf{SNR_F}$ values, $\mu >> 1$, equation (42) can be consequently approximated as

$$\overline{\text{PEP}} \approx \left(2\mu^r\prod_{g=1}^{r}\lambda_g\right)^{-1}. \quad (43)$$

Note that the diversity gain is concluded by r values which is in the range of $[1, n]$. For high $\mathbf{SNR_F}$ values, correct detection of the selected subcarrier indices and a single symbol error detection is expected at the receiver side. In that case, $r = 1$ and terms with higher order can be eliminated from the

above expression. Thus, the asymptotic $\overline{\text{PEP}}$ can be further simplified at high $\mathbf{SNR_F}$ to

$$\overline{\text{PEP}} \approx \frac{1}{2\mu\lambda_1}. \tag{44}$$

To go deeper in the detail of the analysis, several scenarios can be analysed taking into account the possible values of σ_e^2 and κ.

1) IDEAL HARDWARE IMPAIRMENTS AND PERFECT CHANNEL ESTIMATION CASE

$\kappa = 0$ and $\sigma_e^2 = 0$: Consider ideal system where transceiver has ideal hardware and the channel is perfectly known at the receiver. The following conditional PEP is the well-known expression investigated in [5]

$$\Pr\left(X \to \widehat{X}|\widetilde{\boldsymbol{h}}\right) = Q\left(\sqrt{\frac{\mathbf{SNR_F}\left\|(\mathbf{X}-\widehat{\mathbf{X}})\widetilde{\boldsymbol{h}}\right\|^2}{2}}\right). \tag{45}$$

The asymptotic $\overline{\text{PEP}}$ in (44) can be greatly simplified to

$$\overline{\text{PEP}} \approx \frac{2}{\lambda_1 \mathbf{SNR_F}}. \tag{46}$$

Conclusively, increasing $\mathbf{SNR_F}$ enhances the performances of the system.

2) THE PERFECT CHANNEL ESTIMATION CASE

$\sigma_e^2 = 0$ and $\kappa \neq 0$: The conditional upper bound pairwise error probability at perfect CSI case where channel coefficients are totaly predicted and the system is contaminated by hardware impairments is expressed as

$$\Pr\left(X \to \widehat{X}|\widetilde{\boldsymbol{h}}\right) \leq Q\left(\sqrt{\frac{\mathbf{SNR_F}\left\|(\mathbf{X}-\widehat{\mathbf{X}})\widetilde{\boldsymbol{h}}\right\|^2}{2(\mathbf{SNR_F}\kappa^2+1)}}\right). \tag{47}$$

Using the above equation, (44) can be rewritten as

$$\overline{\text{PEP}} \approx \frac{2}{\lambda_1}\left[\kappa^2 + \frac{1}{\mathbf{SNR_F}}\right]. \tag{48}$$

The above expression can be simplified into two cases

$$\overline{\text{PEP}} \approx \begin{cases} \dfrac{2}{\lambda_1 \mathbf{SNR_F}}, & \mathbf{SNR_F} \leq \kappa^2 \\ \dfrac{2}{\lambda_1}\kappa^2, & \mathbf{SNR_F} > \kappa^2 \end{cases}. \tag{49}$$

It can be seen that for $\mathbf{SNR_F}$ value higher than hardware impairment level, the $\overline{\text{PEP}}$ curves saturate to a constant value and an irreducible error floor is manifested.

3) THE PERFECT HARDWARE IMPAIRMENTS CASE

$\kappa = 0$ and $\sigma_e^2 \neq 0$: We assume ideal hardware and that the system is only affected by erroneous channel estimations as narrated in [5]. Hence, (28) is described as

$$\Pr\left(X \to \widehat{X}|\widetilde{\boldsymbol{h}}\right) \leq Q\left(\sqrt{\frac{\mathbf{SNR_F}\left\|(X-\widehat{X})\widetilde{\boldsymbol{h}}\right\|^2}{2(\mathbf{SNR_F}\sigma_e^2+1)}}\right). \tag{50}$$

In such case, the asymptotic $\overline{\text{PEP}}$ is simplified to

$$\overline{\text{PEP}} \approx \frac{2}{\lambda_1}\left[\sigma_e^2 + \frac{1}{\mathbf{SNR_F}}\right]. \tag{51}$$

From the above equation two scenarios can hold attention:

1) In the first scenario, the estimation error is fixed and independent of $\mathbf{SNR_F}$; hence, it can be seen that (51) is not a function of $\mathbf{SNR_F}$ and an error floor is expected in this case, i.e., $\overline{\text{PEP}} \to \frac{2\sigma_e^2}{\lambda_1}$.
2) The estimation error is variable such as $\sigma_e^2 \propto \mathbf{SNR_F}^{-1}$. Under that assumption, the expression in (51) is reduced to

$$\overline{\text{PEP}} \approx \frac{4}{\lambda_1 \mathbf{SNR_F}}. \tag{52}$$

Hence, with increased value of $\mathbf{SNR_F}$ the channel estimation error is reduced and the performances of the system is improved, i.e., there is no error floor.

The calculations in the Rician case follow the same general procedure, except that the numerator of the expression in (37), which is simplified to unity in the Rayleigh case, will be more complicated in the Rician channel. However, in high $\mathbf{SNR_F}$, the expression in (37) can be approximated as in (53), as shown at the bottom of this page.

It can be noticed that the numerator does not depend on $\mathbf{SNR_F}$; therefore, all the results that have been obtained for Rayleigh case can be easily extended to the Rician case. It is obvious now that the line-of-sight component offers a fixed coding gain, but no diversity gain.

D. AVERAGE BIT ERROR PROBABILITY

Te ABEP can be computed using the previous $\overline{\text{PEP}}$ expression as

$$ABEP \approx \frac{1}{bG^{2b}}\sum_{j=1}^{G}\sum_{X}\sum_{\widehat{X}} P(X \to \widehat{X})e(X,\widehat{X}), \tag{54}$$

where $e(X,\widehat{X})$ is the number bit errors related to the $\overline{\text{PEP}}$ event for the j^{th} subblock when X was sent and $\widehat{X}$ received.

$$\overline{\text{PEP}} \approx \frac{\exp\left(-\frac{K}{K+1}\boldsymbol{h}_{dn}^H(X-\widehat{X})^H\left(\frac{1}{K+1}C_{\boldsymbol{h}_{rn}}+\sigma_e^2 I_n\right)^{-1}(X-\widehat{X})\boldsymbol{h}_{dn}\right)}{2\det\left(\mu(X-\widehat{X})\left(\frac{1}{K+1}C_{\boldsymbol{h}_{rn}}+\sigma_e^2 I_n\right)(X-\widehat{X})^H + I_n\right)}. \tag{53}$$

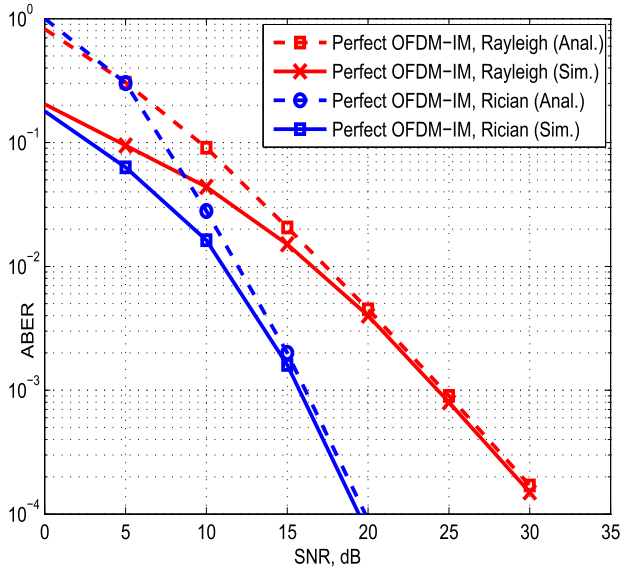

FIGURE 3. Perfect OFDM-IM analytical and simulation average bit error probability with $n = 4$, $k = 2$ using BPSK modulation over Rician ($K = 2$) and Rayleigh fading channels.

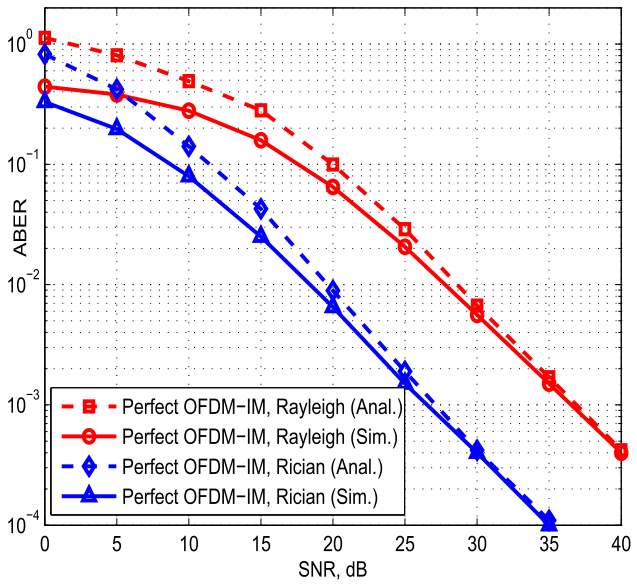

FIGURE 4. Perfect OFDM-IM analytical and simulation average bit error probability with $n = 8$, $k = 6$ using QAM-16 modulation over Rician ($K = 2$) and Rayleigh fading channels.

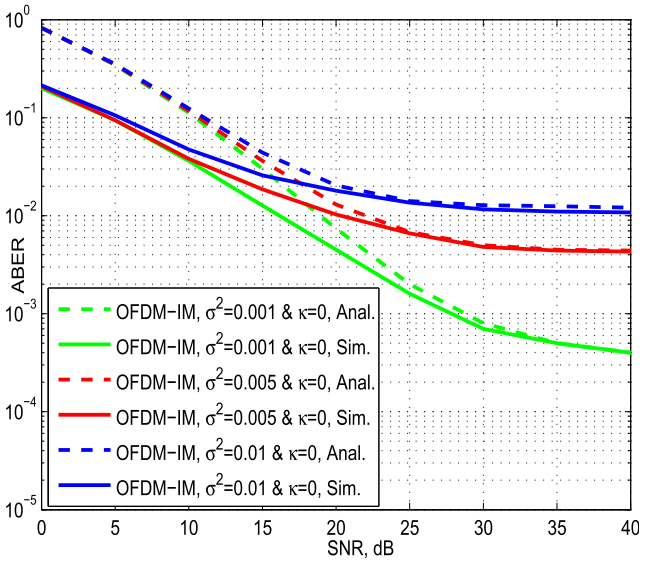

FIGURE 5. OFDM-IM analytical and simulation average bit error probability with $n = 4$, $k = 2$ using BPSK modulation over Rayleigh fading channel for $\sigma_e^2 = [0.001, 0.005, 0.01]$ and $\kappa = 0$.

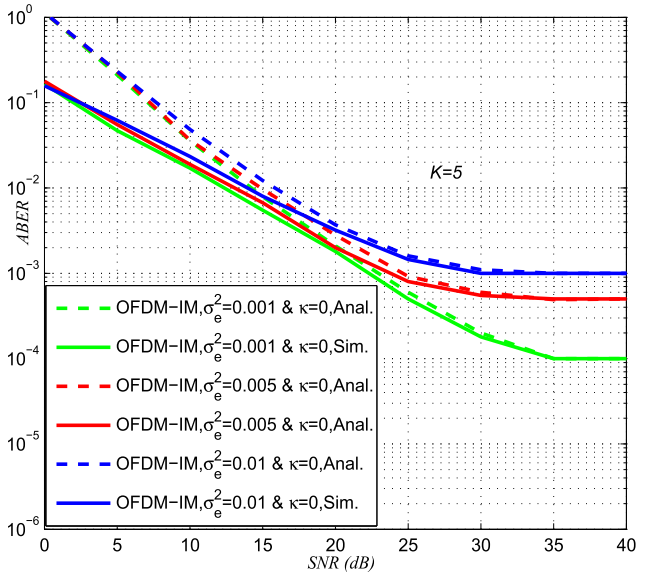

FIGURE 6. OFDM-IM analytical and simulation average bit error probability with $n = 4$, $k = 2$ using BPSK modulation over Rician fading channel (K=5) for $\sigma_e^2 = [0.001, 0.005, 0.01]$ and $\kappa = 0$.

IV. NUMERICAL RESULTS AND DISCUSSIONS

In this section, the depicted expressions of ABER performance in function of $\mathbf{SNR_F}$ highlighting the impacts of hardware impairments and imperfect CSI on OFDM-IM system are carried out over Rician and Rayleigh fading channels. Further, to validate our analysis, the analytical results are compared with Monte-Carlo simulations. The previously discussed scenarios based on κ and σ_e^2 values are adopted in simulations. For clear vision, the case of both ideal hardware and correct channel coefficients estimation over Rician and Rayleigh fading channels, using Binary Phase Shift Keying (BPSK) modulation and $n = 4$, $k = 2$, where n is the number of subcarriers and k is the number of active subcarriersis, is included in Fig. 3. Moreover, the OFDM-IM under ideal conditions is operated for both types of channels over QAM-16 with $n = 8$, $k = 6$ as illustrated in Fig.4. As shown, the analytical result shows perfect match with simulation results for medium to high **SNR** values and OFDM-IM system over Rician channel enhances the Rayleigh fading channel performance.

Fig. 5 and Fig. 6 show the ABER performances of OFDM-IM under ideal hardware and assuming fixed channel

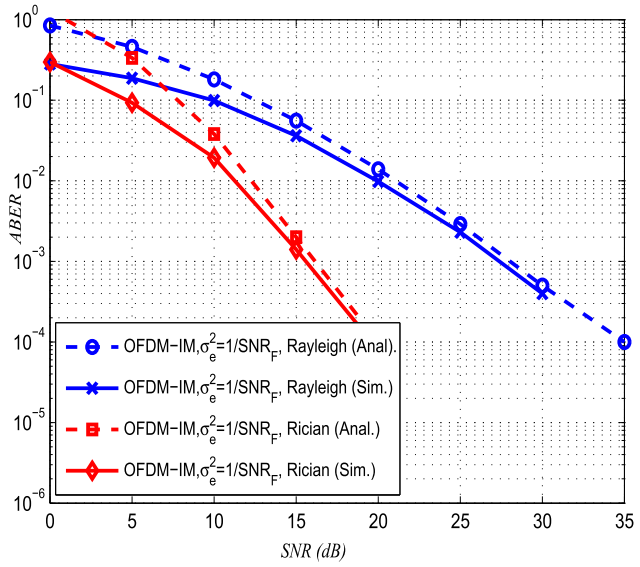

FIGURE 7. OFDM-IM analytical and simulation average bit error probability with $n = 4$, $k = 2$ using BPSK modulation over Rayleigh and Rician fading channels for $\sigma_e^2 = \frac{1}{\mathbf{SNR_F}}$ and $\kappa = 0$.

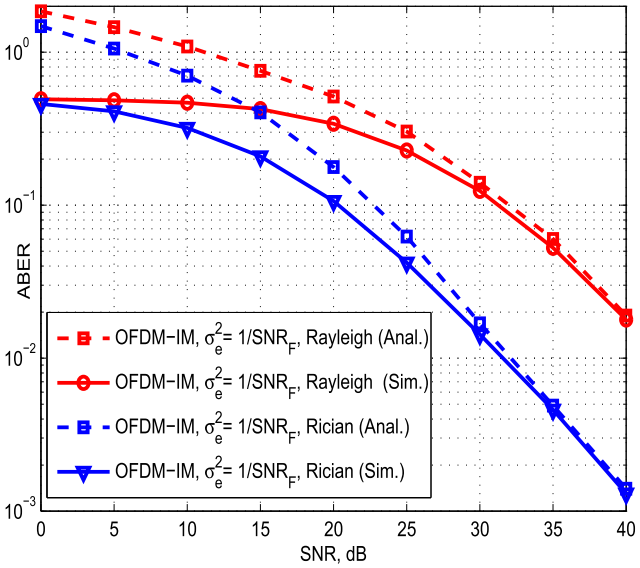

FIGURE 8. OFDM-IM analytical and simulation average bit error probability with $n = 4$, $k = 2$ using QAM-64 modulation over Rayleigh and Rician fading channels for $\sigma_e^2 = \frac{1}{\mathbf{SNR_F}}$ and $\kappa = 0$.

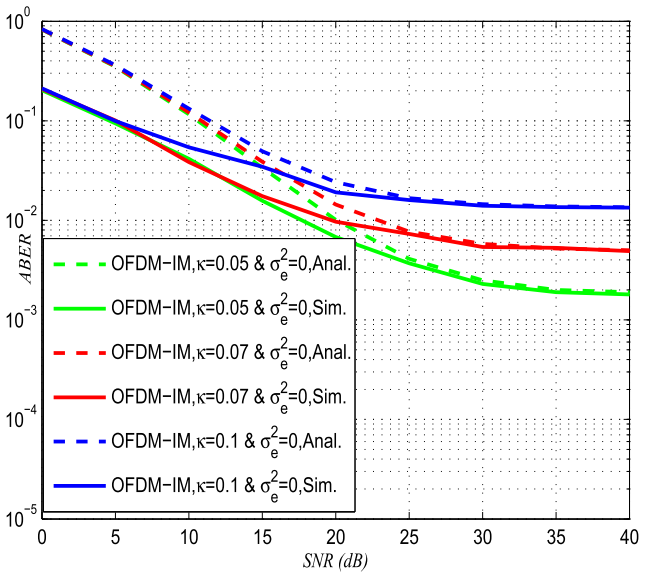

FIGURE 9. OFDM-IM analytical and simulation average bit error probability with $n = 4$, $k = 2$ using BPSK modulation over Rayleigh fading channel for $\sigma_e^2 = 0$ and $\kappa = [0.05, 0.07, 0.1]$.

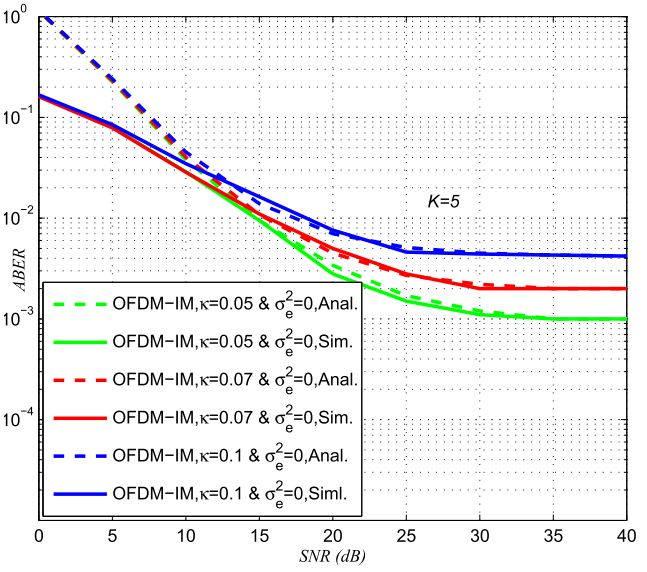

FIGURE 10. OFDM-IM analytical and simulation average bit error probability with $n = 4$, $k = 2$ using BPSK modulation over Rician fading channel for $\sigma_e^2 = 0$ and $\kappa = [0.05, 0.07, 0.1]$.

estimation error over respectively Rayleigh and Rician fading channels. It is apparent that increasing the σ_e^2 value from 0.001 to 0.01 harmfully affects the ABER performance of the system for both types of channels. An irreducible error floor comes into sight at high **SNR** due to the constant channel error which is independent of **SNR**. Unlike traditional spatial modulation and quadrature spatial modulation, as the Rician factors increase the error probability decreases. Further, the analytical analysis is very close to the simulation results, which validates the proposed analysis.

When the variance of the Gaussian estimation errors decreases and the $\mathbf{SNR_F}$ of the data symbols increases (the pilot symbols have the same energy as the data symbols) that is $\sigma_e^2 = \frac{1}{\mathbf{SNR_F}}$, we observe that no error floor exists as shown in Fig. 7 using BPSK modulation and in Fig.8 using QAM-64. Finally, it should be noted that the tightness of error performance improves as **SNR** increases; however, the proposed analysis slightly loses its tightness at low **SNR** values.

In Fig. 9 and Fig. 10, the ABER performances of OFDM-IM over Rayleigh and Rician fading channels

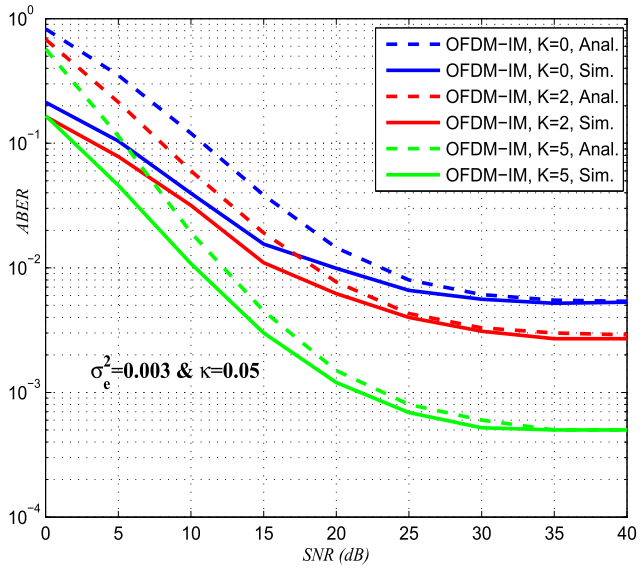

FIGURE 11. OFDM-IM analytical and simulation average bit error probability with $n = 4$, $k = 2$ using BPSK modulation over Rician fading channel for $\sigma_e^2 = 0.003$ and $\kappa = 0.05$ with varied K.

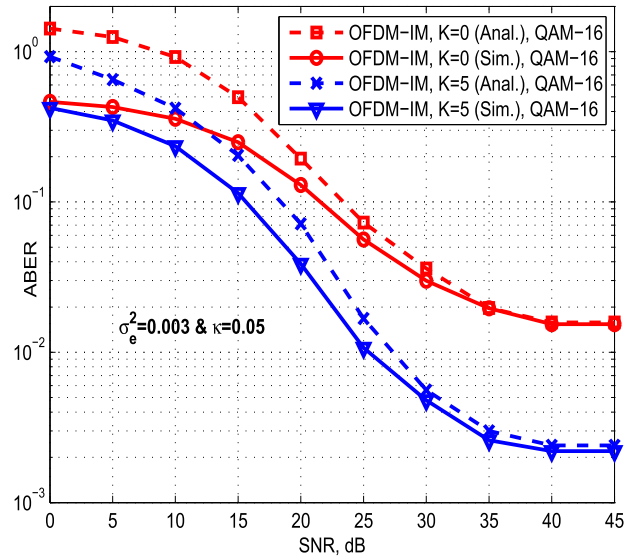

FIGURE 12. OFDM-IM analytical and simulation average bit error probability with $n = 8$, $k = 6$ using QAM-16 modulation over Rician fading channel for $\sigma_e^2 = 0.003$ and $\kappa = 0.05$ with $K = \{0, 5\}$.

under hardware impairments and perfect channel estimation are investigated. Simulation and numerical results were concluded under different hardware impairments levels, $\kappa = [0.05, 0.07, 0.1]$. As observed here, the ABER performance decays at a higher value of κ. As expected, at high **SNR**, an error floors appear due to the considered hardware impairments level.

The impact of the Rician K factor on the performance of OFDM-IM system is carried under fixed hardware impairments level $\kappa = 0.05$ and imperfect channel knowledge channel with $\sigma_e^2 = 0.003$. Different values for K parameters from 0 to 5 are presented in Fig. 11 using BPSK modulation with $n = 4$, $k = 2$ and in Fig.12 using QAM-16 modulation with $n = 8$, $k = 6$. The value of $K = 0$ presents the Rayleigh fading channel case. Increasing the value of K boost the performance of OFDM-IM system as depicted in Fig. 11. This improvement affects the coding gain, not the diversity gain.

Conclusively, the performance of OFDM-IM deteriorates with the presence of imperfect hardware and/or channel parameters estimation notably in high **SNR** regions. Accordingly, assuming perfect cases does not allow any realistic configuration.

V. CONCLUSION

This paper investigates the destructive effects of the joint presence of hardware impairments and channel estimation errors on OFDM-IM system over correlated fading channels. Simulation results coincide with the reported results for both Rician and Rayleigh fading channels and hence confirm the proposed analytical expressions for different scenarios. Therefore, the announced generalized model is an adequate platform for high data rate wireless communication system implementation in the condition of using imperfect CSI and hardware impairments mitigation techniques which will be developed in future works.

REFERENCES

[1] R. Abu-Alhiga and H. Haas, "Subcarrier-index modulation OFDM," in *Proc. IEEE Int. Symp. Pers., Indoor Mobile Radio Commun.*, Tokyo, Japan, Sep. 2009, pp. 177–181.

[2] D. Tsonev, S. Sinanovic, and H. Haas, "Enhanced subcarrier index modulation (SIM) OFDM," in *Proc. IEEE GLOBECOM Workshops*, Dec. 2011, pp. 728–732.

[3] R. Y. Mesleh, H. Haas, S. Sinanovic, C. W. Ahn, and S. Yun, "Spatial modulation," *IEEE Trans. Veh. Technol.*, vol. 57, no. 4, pp. 2228–2241, Jul. 2008.

[4] E. Başar, Ü. Aygölü, E. Panayırcı, and H. V. Poor, "Space-time block coded spatial modulation," *IEEE Trans. Commun.*, vol. 59, no. 3, pp. 823–832, Mar. 2011.

[5] E. Başar, Ü. Aygölü, E. Panayırcı, and H. V. Poor, "Orthogonal frequency division multiplexing with index modulation," *IEEE Trans. Signal Process.*, vol. 61, no. 22, pp. 5536–5549, Nov. 2013.

[6] E. Başar, Ü. Aygölü, E. Panayırcı, and H. V. Poor, "Performance of spatial modulation in the presence of channel estimation errors," *IEEE Commun. Lett.*, vol. 16, no. 2, pp. 176–179, Feb. 2012.

[7] C. Kong, C. Zhong, A. K. Papazafeiropoulos, M. Matthaiou, and Z. Zhang, "Effect of channel aging on the sum rate of uplink massive MIMO systems," in *Proc. IEEE Int. Symp. Inf. Theory (ISIT)*, Jun. 2015, pp. 1222–1226.

[8] T. Weber, A. Sklavos, and M. Meurer, "Imperfect channel-state information in MIMO transmission," *IEEE Trans. Commun.*, vol. 54, no. 3, pp. 543–552, Mar. 2006.

[9] C. H. Yih, "Effects of channel estimation error in the presence of CFO on OFDM BER in frequency-selective Rayleigh fading channels," *J. Commun.*, vol. 3, no. 3, pp. 10–18, 2008.

[10] V. Tarokh, A. Naguib, N. Seshadri, and A. R. Calderbank, "Space-time codes for high data rate wireless communication: Performance criteria in the presence of channel estimation errors, mobility, and multiple paths," *IEEE Trans. Commun.*, vol. 47, no. 2, pp. 199–207, Feb. 1999.

[11] C. Muschallik, "Influence of RF oscillators on an OFDM signal," *IEEE Trans. Consum. Electron.*, vol. 41, no. 3, pp. 592–603, Aug. 1995.

[12] L. Tomba, "On the effect of Wiener phase noise in OFDM systems," *IEEE Trans. Commun.*, vol. 46, no. 5, pp. 580–583, May 1998.

[13] E. Costa, M. Midrio, and S. Pupolin, "Impact of amplifier nonlinearities on OFDM transmission system performance," *IEEE Commun. Lett.*, vol. 3, no. 2, pp. 37–39, Feb. 1999.
[14] D. Dardari, V. Tralli, and A. Vaccari, "A theoretical characterization of nonlinear distortion effects in OFDM systems," *IEEE Trans. Commun.*, vol. 48, no. 10, pp. 1755–1764, Oct. 2000.
[15] A. Schuchert, R. Hasholzner, and P. Antoine, "A novel IQ imbalance compensation scheme for the reception of OFDM signals," *IEEE Trans. Consum. Electron.*, vol. 47, no. 3, pp. 313–318, Aug. 2001.
[16] H. Liu and U. Tureli, "A high-efficiency carrier estimator for OFDM communications," *IEEE Commun. Lett.*, vol. 2, no. 4, pp. 104–106, Apr. 1998.
[17] S. G. Domouchtsidis, G. D. Ntouni, V. M. Kapinas, and G. K. Karagiannidis, "OFDM-IM vs FQAM: A comparative analysis," in *Proc. IEEE Int. Telecommun. (ICT)*, May 2016, pp. 1–5.
[18] C. Studer, M. Wenk, and A. Burg, "MIMO transmission with residual transmit-RF impairments," in *Proc. ITG/IEEE WSA*, Feb. 2010, pp. 189–196.
[19] T. Schenk, *RF Imperfections in High-rate Wireless Systems: Impact and Digital Compensation*. New York, NY, USA: Springer, 2008.
[20] P. Zetterberg, "Experimental investigation of TDD reciprocity-based zero-forcing transmit precoding," *EURASIP J. Adv. Signal Process.*, vol. 2011, Jan. 2011, Art. no. 137541.
[21] E. Björnson, J. Hoydis, M. Kountouris, and M. Debbah, "Hardware impairments in large-scale MISO systems: Energy efficiency, estimation, and capacity limits," in *Proc. IEEE 18th Int. Conf. Digit. Signal Process. (DSP)*, Fira, Greece, Jul. 2013, pp. 1–6.
[22] M. Matthaiou, A. Papadogiannis, E. Björnson, and M. Debbah, "Two-way relaying under the presence of relay transceiver hardware impairments," *IEEE Commun. Lett.*, vol. 17, no. 6, pp. 1136–1139, Jun. 2013.
[23] E. Björnson, P. Zetterberg, and M. Bengtsson, "Optimal coordinated beamforming in the multicell downlink with transceiver impairments," in *Proc. IEEE GLOBECOM*, Dec. 2012, pp. 4775–4780.
[24] "8 hints for making and interpreting EVM measurements," Agilent Technol., Santa Clara, CA, USA, Appl. Note, 2005.
[25] A. Afana and S. Ikki, "Analytical framework for space shift keying MIMO systems with hardware impairments and co-channel interference," *IEEE Commun. Lett.*, vol. 21, no. 3, pp. 488–491, Mar. 2017.
[26] E. Björnson, M. Matthaiou, and M. Debbah, "A new look at dual-hop relaying: Performance limits with hardware impairments," *IEEE Trans. Commun.*, vol. 61, no. 11, pp. 4512–4525, Nov. 2013.
[27] M. K. Simon and M.-S. Alouini, *Digital Communication Over Fading Channels: A Unified Approach to Performance Analysis*. New York, NY, USA: Wiley, 2000.
[28] M. K. Simon and D. Divsalar, "Some new twists to problems involving the Gaussian probability integral," *IEEE Trans. Commun.*, vol. 46, no. 2, pp. 200–210, Feb. 1998.
[29] V. V. Veeravalli, "On performance analysis for signaling on correlated fading channels," *IEEE Trans. Commun.*, vol. 49, no. 11, pp. 1879–1883, Nov. 2001.
[30] M. Chiani and D. Dardari, "Improved exponential bounds and approximation for the Q-function with application to average error probability computation," in *Proc. IEEE Global Telecommun. Conf.*, vol. 2. Bologna, Italy, Nov. 2002, pp. 1399–1402.
[31] M. S. Alouini and A. J. Goldsmith, "A unified approach for calculating error rates of linearly modulated signals over generalized fading channels," *IEEE Trans. Commun.*, vol. 47, no. 9, pp. 1324–1334, Sep. 1999.

ASMA BOUHLEL received the Diploma degree in electrical engineering and the M.S. degree from the National Engineering School of Monastir, in 2011 and 2013, respectively, where she is currently pursuing the Ph.D. degree in electrical engineering. Her research interests include signal processing for wireless communications, multiple-input multiple-output systems, spatial modulation systems, and orthogonal frequency division multiplexing with index modulation. In 2018, she has obtained a scholarship for a Post-Doctorate Fellow position at Lakehead University, Canada.

STAVROS G. DOMOUCHTSIDIS received the M.Eng. degree in electrical and computer engineering with a specialization in the field of telecommunications from the Aristotle University of Thessaloniki, Greece, in 2016. He is currently pursuing the Ph.D. degree in computer science with the Interdisciplinary Centre for Security, Reliability and Trust, University of Luxembourg. His research interests are in signal processing for wireless communications, focusing on multicarrier systems, large scale antenna systems, and interference mitigation techniques for MIMO communications.

SALAMA S. IKKI received the B.S. degree from Al-Isra University, Amman, Jordan, in 1996, the M.Sc. degree from the Arab Academy for Science and Technology and Maritime Transport, Alexandria, Egypt, in 2002, and the Ph.D. degree from the Memorial University of Newfoundland, St. John's, in 2009, all in electrical engineering. He was a Research Assistant with the INRS, University of Quebec, Montreal, from 2010 to 2012 and a Post-Doctoral Fellow with the University of Waterloo, Waterloo, ON, Canada, from 2009 to 2010. He is currently an Associate Professor in wireless communications with the Department of Electrical Engineering, Lakehead University. He has been carrying out research in communications and signal processing for over ten years. He is widely recognized as an expert in the field of wireless communications. He has authored or co-authored over 100 papers in peer-reviewed IEEE international journals and conferences with over 3000 citations and has a current h-index of 30. He was a recipient of the Best Paper Award published in the *EURASIP Journal on Advances in Signal Processing*, the IEEE Communication Letters, and the IEEE Wireless Communication Letters Exemplary Reviewer Certificate in 2012, and the Top Reviewer Certificate from the IEEE Transaction on Vehicular Technology in 2015. His Ph.D. student received the second place for the Best Poster from the School of Electrical and Electronic Engineering, Newcastle University, U.K., Annual Research Conference, in 2014. He serves on the Editorial Board of the IEEE Communication Letters and the *IET Communications Proceeding*.

ANIS SAKLY has received the Diploma degree in electrical engineering from the National Engineering School of Monastir (ENIM) in 1994, and the Ph.D. degree in electrical engineering from the National Engineering School of Tunis in 2005. He is currently a Professor with ENIM. His research interests are in the analysis and synthesis of intelligent control systems, particularly soft computing-based control approaches.